NATIONAL HURRICANE RESEARCH PROJECT

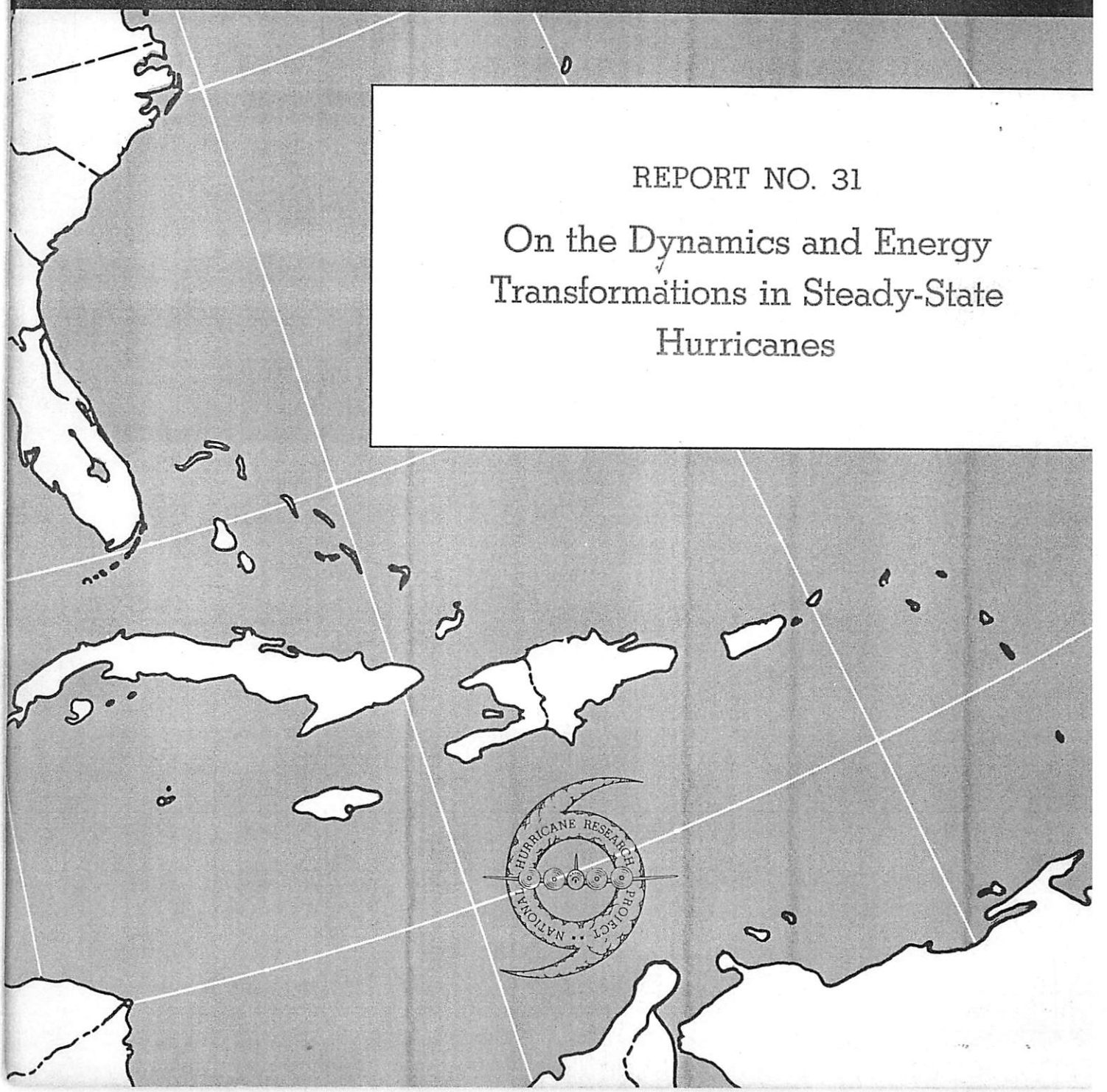

REPORT NO. 31

On the Dynamics and Energy Transformations in Steady-State Hurricanes

U. S. DEPARTMENT OF COMMERCE
Frederick H. Mueller, Secretary
WEATHER BUREAU
F. W. Reichelderfer, Chief

NATIONAL HURRICANE RESEARCH PROJECT

REPORT NO. 31

On the Dynamics and Energy Transformations in Steady-State Hurricanes*

by
J. S. Malkus
Woods Hole Oceanographic Institution
and
H. Riehl
The University of Chicago

*Contribution No. 1034 from the Woods Hole Oceanographic Institution

Washington, D. C.
September 1959

NATIONAL HURRICANE RESEARCH PROJECT REPORTS

Reports by Weather Bureau units, contractors, and cooperators working on the hurricane problem are pre-printed in this series to facilitate immediate distribution of the information among the workers and other interested units. As this limited reproduction and distribution in this form do not constitute formal scientific publication, reference to a paper in the series should identify it as a pre-printed report.

No. 1. Objectives and basic design of the NHRP. March 1956.
No. 2. Numerical weather prediction of hurricane motion. July 1956.
Supplement: Error analysis of prognostic 500-mb. maps made for numerical weather prediction of hurricane motion. March 1957.
No. 3. Rainfall associated with hurricanes. July 1956.
No. 4. Some problems involved in the study of storm surges. December 1956.
No. 5. Survey of meteorological factors pertinent to reduction of loss of life and property in hurricane situations. March 1957.
No. 6. A mean atmosphere for the West Indies area. May 1957.
No. 7. An index of tide gages and tide gage records for the Atlantic and Gulf coasts of the United States. May 1957.
No. 8. Part I. Hurricanes and the sea surface temperature field.
Part II. The exchange of energy between the sea and the atmosphere in relation to hurricane behavior. June 1957.
No. 9. Seasonal variations in the frequency of North Atlantic tropical cyclones related to the general circulation. July 1957.
No. 10. Estimating central pressure of tropical cyclones from aircraft data. August 1957.
No. 11. Instrumentation of NHRP aircraft. August 1957.
No. 12. Studies of hurricane spiral bands as observed on radar. September 1957.
No. 13. Mean soundings for the hurricane eye. September 1957.
No. 14. On the maximum intensity of hurricanes. December 1957.
No. 15. The three-dimensional wind structure around a tropical cyclone. Jan.1958.
No. 16. Modification of hurricanes through cloud seeding. May 1958.
No. 17. Analysis of tropical storm Frieda, 1957. A preliminary report.June 1958.
No. 18. The use of mean layer winds as a hurricane steering mechanism.June 1958.
No. 19. Further examination of the balance of angular momentum in the mature hurricane. July 1958.
No. 20. On the energetics of the mature hurricane and other rotating wind systems. July 1958.
No. 21. Formation of tropical storms related to anomalies of the long-period mean circulation. September 1958.
No. 22. On production of kinetic energy from condensation heating. October 1958.
No. 23. Hurricane Audrey storm tide. October 1958.
No. 24. Details of circulation in the high energy core of hurricane Carrie. November 1958.
No. 25. Distribution of surface friction in hurricanes. November 1958.
No. 26. A note on the origin of hurricane radar spiral bands and the echoes which form them. February 1959.
No. 27. Proceedings of the Board of Review and conference on research progress. March 1959.
No. 28. A model hurricane plan for a coastal community. March 1959.
No. 29. Exchange of heat, moisture and momentum between hurricane Ella (1958) and its environment. April 1959.
No. 30. Mean soundings for the Gulf of Mexico Area. April 1959.

CONTENTS

ON THE DYNAMICS AND ENERGY TRANSFORMATIONS IN STEADY-STATE HURRICANES

J. S. Malkus
Woods Hole Oceanographic Institution

and

H. Riehl
The University of Chicago

[Manuscript received June 9, 1959]

ABSTRACT

A dynamic model of the inflow layer in a steady mature hurricane is evolved, relating wind speed, pressure gradient, surface shearing stress, mass flow, and convergence. The low-level air trajectories are assumed to be logarithmic spirals. With this hypothesis, properties such as maximum wind and central pressure are determined through choice of a parameter depending on the inflow angle: a moderate hurricane arises with inflow angles of about 20°, while 25° gives an intense or extreme storm.

Most of this study treats the moderate storm. In order to maintain its core pressure gradients, an oceanic source of sensible and latent heat is required. As a result, latent heat release in the inner hurricane area occurs at higher heat content (warmer moist adiabats) than mean tropical subcloud air. The heat transfer from the ocean and the release of latent heat in the core determine the pressure gradient along the trajectory, and this prescribes the particular trajectory selected by the air among an infinite number available from the logarithmic spiral family.

This selection principle is evolved using recent work on "relative stability" of finite amplitude thermal circulations. Of an infinite number of dynamically possible spirals, the one is realized which maximizes the rate of kinetic energy production under the thermodynamic constraints, here formulated in terms of the relation between heat release and pressure gradient.

Finally, rainfall, efficiency of work done by the storm, and kinetic energy budgets are examined in an attempt to understand the difference between the hurricane - a rare phenomenon - and the common sub-hurricane tropical storm.

1. INTRODUCTION

The tropical hurricane is a thermally driven circulation whose primary energy source is release of latent heat of condensation. This heating acts to establish the pressure gradients which produce and maintain hurricane winds. Radar photographs, since the early 1940's, have demonstrated abundantly that latent heat is not released uniformly through the rain area, but that it is concentrated in spiral convective bands of narrow width and especially in a central ring surrounding the eye (Maynard [12], Wexler [22]). In this paper the low-level air along an inward spiralling convective band will be followed from the outskirts to the eye. The purpose is to begin a study of the mechanisms by which energy release along such a path is utilized to maintain the pressure field of a mature storm in steady state.

Large pressure gradients are required to sustain a narrow ring of hurricane winds, with order of 30 mb. in 60 km. The central pressure of a hurricane of moderate strength must be about 960 mb., 4-5 percent below mean sea level pressure. Available evidence suggests that this substantial reduction is brought about by tropospheric heating, and that an undisturbed top may be assumed within the limits of interest in this investigation. As demonstrated by Haurwitz [5], pressures in hurricanes are very nearly hydrostatic and, given a fixed top, lateral pressure gradients are produced by density variations within the troposphere. Such variations may result from release of latent heat in the precipitation area and from dry-adiabatic sinking in the eye.

Formerly it was held that an outward slope of the eye wall with height could explain the low pressures in the inner convective ring around the eye. According to Malkus [10], the slope of the cumulonimbi forming the eye wall is governed by the factors generally determining the slant of such clouds. From consideration of cloud dynamics and angular momentum constraints, an eye wall is prevented from slanting more than 45°-60° from the vertical. Since the height of the cumulonimbi is 10-14 km., this means that, in a storm with eye radius of 20-30 km., the eye slope can at most account for rain area pressures to distances of 30-40 km. from the center. Extensive photography of eye walls by the National Hurricane Research Project of the U. S. Weather Bureau and various radar studies have demonstrated that such large slopes are rarely, if ever, realized; these data suggest that, more likely, the eye wall is nearly perpendicular.

Hence, the contribution of dry-adiabatic sinking to lateral density gradients in the rain area may be neglected. It is assumed that the whole density gradient is derived from latent heat release; further that the cloud towers are nearly vertical to about 9-10 km. altitude. In the high troposphere the mass ascending in the cumulonimbi converges vertically and spreads laterally covering large horizontal areas. Although the winds turn with height in this layer, often sharply, we assume as a first approximation that the air above the vertical portion of a cumulonimbus has the same properties as would have been obtained from continued vertical ascent to the top of the convective layer. Thus the surface pressure at any point may be computed hydrostatically from the ascent path of the surface air to the high troposphere.

The warmest possible ascent of normal tropical air lies along the moist adiabat with equivalent potential temperature (θ_E) of about 350°A. If the top

of the circulation is taken at 150 mb. at standard height for the Caribbean area in summer, the lowest surface pressure obtained through this ascent will be about 1000 mb. from the hydrostatic equation (Riehl [15]). This is a threshold value, and it is interesting to note that many tropical storms reach equilibrium at this central pressure. The total heat content of normal tropical air, raised undilute (without entrainment) to the level of zero buoyancy, is insufficient to generate pressures substantially below 1000 mb. It follows that a local heat source must exist within hurricanes to permit increases of θ_E of the surface air above 350°A. The existence of such a heat source has been inferred by Byers [1] and demonstrated to exist from surface observations (Riehl [15]).

It also follows that variations in the rate of import, condensation, and export of normal tropical air will not lead to variations in surface pressure because the ascent path, and therewith the density of the vertical column, is entirely determined by the θ_E of the rising air. A storm will not deepen if simply more water is condensed at θ_E = 350°A in the core; it can do so only if there is an additional heat source so that condensation will occur at θ_E greater than 350°A.*

As first step, the surface pressure was computed from a series of moist adiabats with the foregoing model, namely that vertical ascent can be assumed to the level of zero buoyancy. The undisturbed top was taken as 100 mb. and a mean tropical atmosphere (Jordan [8]) was used for the layer between 100 mb. and the pressure at zero buoyancy. For moist adiabatic ascents between θ_E = 350°A. and 365°A., surface pressure (p_s) and θ_E are related linearly. One obtains

$$- \delta p_s = 2.5 \, \delta\theta_E \, . \qquad (1)$$

Following this relation, the sea level pressure will drop about 12.5 mb. for an increase of 5°A. in θ_E. Suppose that the oceanic heat source begins to become effective at p_s = 1000 mb. with θ_E = 350°A. Then, if the increment in θ_E is 15°A., the central pressure will be 962.5 mb. at θ_E = 365°A. This rise in θ_E corresponds to an increase of the heat content of the surface air of 3-4 cal./gm. which must be absorbed from the ocean if ascent at 365°A. is to occur. The question is whether in reality such a heat exchange can be realized. In the following a dynamical model will be developed for the inflow layer which will permit computation of the pressure drop required for a steady-state vortex. Then, from estimates of heat exchange between sea and air, it will be determined whether this pressure decrease is consistent with equation (1).

*It should be noted, however, that in cases when mid-tropospheric air not derived from the surface enters the rain area (Simpson and Riehl [21]) with characteristic θ_E of only 330°-340°A., an increased rate of surface mass inflow at 350°A. will act to maintain the heat content of a storm's interior. The constraint upon hurricane growth and maintenance arising from such lateral "ventilation" will be considered in subsequent publications.

2. A DYNAMIC MODEL OF THE LOW-LEVEL RAIN AREA

The inflow into a hurricane is confined mainly to low levels. Subcloud air is accelerated inward along spiral-shaped trajectories; acceleration results from excess work done by pressure gradient forces over frictional retardation. We shall consider the dynamics of the inflow layer in a natural coordinate framework, found useful in studies of other types of thermal circulations (Riehl et al. [20], Malkus [9], Riehl and Fultz [17]). This coordinate system, superposed on cylindrical coordinates is illustrated in figure 1, where s is distance along the trajectory, n is the normal coordinate and z the vertical coordinate, directed to form a right-handed system. The crossing angle between trajectory and circles of equal radius r from the storm center 0 is denoted by β; the radius of curvature of the trajectories is R. The tangential and normal equations of motion to be used are as follows:

$$\frac{dv}{dt} \cong v\frac{\partial v}{\partial s} = -\frac{1}{\rho}\frac{\partial p}{\partial s} + \frac{1}{\rho}\frac{\partial \tau_{sz}}{\partial z} = \frac{1}{\rho}\frac{\partial p}{\partial r}\sin\beta + \frac{1}{\rho}\frac{\partial \tau_{sz}}{\partial z} \qquad (2)$$

$$\frac{v^2}{R} + fv = -\frac{1}{\rho}\frac{\partial p}{\partial n} = \frac{1}{\rho}\frac{\partial p}{\partial r}\cos\beta \qquad (3)$$

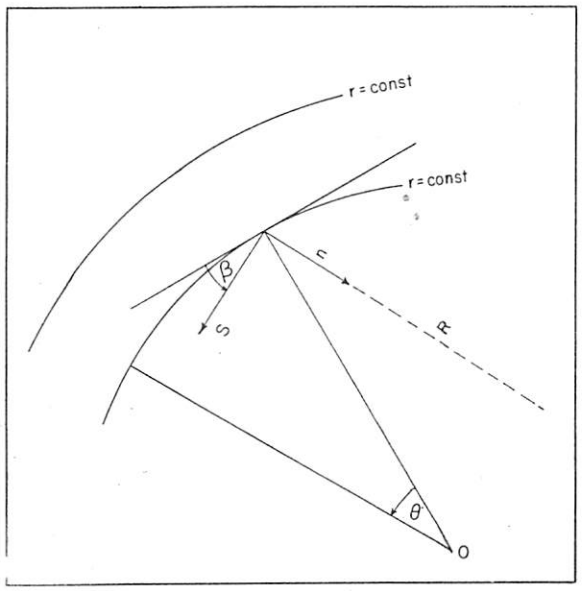

Figure 1. - Coordinate system used for hurricane models. Origin at 0. r and θ form a standard cylindrical system. The direction s is chosen along the trajectories, positive downstream, with n the normal coordinate. β is the inflow or "crossing" angle formed between s and circles of constant radius. R is the radius of curvature of the trajectories.

Here t is time, r the radial coordinate, v velocity, p pressure, ρ density, f the Coriolis parameter, and τ_{sz} the shearing stress component transferring s-momentum along the vertical.

Assumptions introduced so far are as follows:

(1) The storm is in steady state, either stationary or very slowly moving.

(2) The pressure field is radially nearly symmetrical, i.e. $\frac{\partial p}{r\partial\theta} \ll \frac{\partial p}{\partial r}$. Since all other quantities may vary from one trajectory to the next, and thence with azimuth angle θ, this choice does not restrict the applicability of the model to symmetrical circulations.

(3) The vertical transport of s-momentum by the mean motion, $w\frac{\partial v}{\partial z}$ (w is the vertical velocity component) is small compared to $v\frac{\partial v}{\partial s}$. This assumption is valid because the vertical motion is zero at the ground and $\frac{\partial v}{\partial z}$ is small

throughout the inflow layer except quite close to the ground. Vertical momentum transport by convective-scale elements is included in the shearing stress term.

(4) Lateral turbulent transport of s-momentum is neglected compared to vertical transport with the hypothesis that momentum from the air inside the hurricane is abstracted by the ocean and not diffused laterally outward by small-scale eddies. This assumption is probably weak if single trajectories or only small segments of a storm are considered, but due to the difficulty of prescribing the vertical eddy transport accurately, is not critical at present.

(5) The wind direction is nearly constant with height through the inflow layer so that the shearing stress term $\frac{\partial \tau_{nz}}{\partial z}$ may be omitted.

We shall now substitute $\frac{r}{\cos\beta}$ for R, the radius of trajectory curvature in (3). This is exact for the logarithmic spiral where $\cos\beta$ = constant and nearly true when the inflow angle varies slowly along the trajectory. When $\beta \approx 20°$ or less, R differs from r by only about 6 percent for any trajectory. Let equation (2) be multiplied by $\cos\beta$ and equation (3) by $\sin\beta$. The pressure gradient force is then eliminated by combining these equations and we have, after dividing again by $\cos\beta$,

$$\frac{v^2}{r}\sin\beta + fv\tan\beta - v\frac{\partial v}{\partial s} = -\frac{1}{\rho}\frac{\partial \tau_{sz}}{\partial z} \qquad (4)$$

Upon averaging vertically through the inflow layer of height δz, we have

$$\tilde{\rho}\delta z\left[\frac{\tilde{v}^2}{r}\sin\beta + f\tilde{v}\tan\beta - \tilde{v}\frac{\partial \tilde{v}}{\partial s}\right] = \tau_{so} = K_F \rho_o v_o^2, \qquad (5)$$

using the commonly assumed dependence of τ_{so} upon the square of the surface wind. The symbol $\sim$ denotes vertical averaging, K_F is an empirically determined coefficient, and the subscript zero denotes surface properties. We shall neglect the slight difference between ρ_o and $\tilde{\rho}$, also between $\tilde{v}$ and v_o, since the vertical shear above anemometer level generally is considered to be very weak in the interior of hurricanes, especially over water. The important assumption in going from the right side of equation (4) to that of equation (5) is that the shearing stress vanishes at the top of the inflow layer in accord with the hypothesis that $\frac{\partial v}{\partial z}$ is very weak above the ground layer. In the remainder of this section only quantities averaged through the inflow layer will be considered and the symbol $\sim$ will again be omitted for convenience.

Dividing out a v and utilizing the definition that $\frac{\partial v}{\partial s} = -\frac{\partial v}{\partial r}\sin\beta$, we derive the following first-order differential equation for the velocity v along any trajectory as a function of radial distance r from the storm center,

$$\frac{dv}{dr} + v \left[\frac{1}{r} - \frac{K_F}{\sin\beta\, \delta z} \right] = - \frac{f}{\cos\beta} \qquad (6)$$

Since it will prove more convenient to set boundary conditions on v_θ, the tangential velocity component, we may obtain an equation for it by using the fact that $v = \frac{v_\theta}{\cos\beta}$, namely

$$\frac{dv_\theta}{dr} + v_\theta \left[\frac{1}{r} + C(r) \right] = - f \qquad (7)$$

where $C(r) = \frac{-K_F}{\sin\beta\, \delta z}$.

It should be noted that equation (7) specifies the dependence of v upon r for a single trajectory; it may be integrated separately for one or more trajectories within a single storm or for the mean trajectories of several storms. Whichever is done, the difference between trajectories is determined by the parameter C(r). Equation (7) may be integrated analytically if C(r) is a constant or varies in some simple manner with the radius. Numerical integration may be undertaken if it should prove desirable to treat a complex dependence of C upon r.

The results of Palmén and Riehl [14] suggest that although K_F and δz may each vary by a factor of two under hurricane conditions (increasing inward) their ratio is constant within 20 percent. We chose $K_F/\delta z = 1.36 \times 10^{-8}$ cm.$^{-1}$ for the following analysis, which permits K_F to vary from 1.1 to 3.0×10^{-3} for a range of the depth of the inflow layer from 750 m. to 2.2 km.

We shall make the simplest possible choice of β for our trajectory calculations, namely $\beta = \beta_L$ = constant for the outer rain area, $r > 100$ km. and decreasing from there linearly to zero at r = 25 km., the assumed radius of the eye wall. The solution to (7) is thus an infinite family of simple logarithmic spirals (modified slightly in the interior) each differing from the others by means of a different inflow angle β.

Integrating equation (7) when C(r) = constant,

$$v_\theta\, r = \frac{f}{C^2} (1 - Cr) + C_1\, e^{-Cr}. \qquad (8)$$

An outer boundary condition must be applied to evaluate the constant of integration C_1. This will be done by choosing an outer radius r_o where the relative vorticity vanishes, that is $\frac{dv_\theta}{dr} + \frac{v_\theta}{r} = 0$. Since $v_r = v_\theta \tan\beta$, v_r also satisfies this relation at r_o, which thus separates the region of inner horizontal convergence from outer horizontal divergence. Choice of r_o is arbitrary, but the computed structure of the storm core is not sensitive

to this choice as long as $r_o \geq 500$ km. For moderate hurricanes such as Carrie (September 15, 1957) and Daisy (August 27, 1958), data from the National Hurricane Research Project of the U. S. Weather Bureau suggest that $r_o \cong 500$ km. is satisfactory. For bigger storms, such as some Pacific typhoons, r_o might be 800-1000 km.

When the outer boundary condition is applied, $C_1 = \frac{-f}{C^2} e^{Cr_o}$ and

$$v_\theta r = \frac{f}{C^2} [1 - Cr - e^{C(r_o - r)}] . \qquad (9)$$

For the inner rain area, namely $r_E < r < r_1$ where r_1 is 100 km. and r_E, the eye boundary, is 25 km., we choose

$$\sin\beta = (\sin\beta_L) \frac{r - r_E}{r_1 - r_E} .$$

Equation (7) may be solved exactly under this assumption, matching v at r_1 = 100 km. However, near the core Coriolis forces are negligible compared to centrifugal, leaving only the homogeneous part of the equation. This yields a simple solution for the inner rain area,

$$v_\theta r = C_2 [r - r_E]^{-(r_1 - r_E) C} \qquad (10)$$

where C_2 is obtained by matching v_θ at 100 km. with the results of (9).

We now calculate two model hurricane trajectories at latitude 20°, a moderate and an intense one, with r_o = 500 km. in both cases. The only difference between them lies in the choice of sin β_L, which for the moderate trajectory is 0.342 (β_L = 20°); and for the intense hurricane sin β_L = 0.423 (β_L = 25°). The other parameters such as ρ, f, $\frac{K_F}{\delta z}$, r_1, and r_E are the same for both cases, with values as noted. Tangential speed as a function of radius in the two situations is given in table 1.

The results of this table can be regarded as applying to single trajectories within a storm or storms, or to a mean trajectory; in the latter case v_θ represents the azimuth-averaged tangential wind speed for an entire hurricane. Highest wind speed is about 112 knots for case A which will be called "moderate storm." In case B, 175 knots are attained. This range of maximum wind is realistic, as is also the distribution of v_θ with radius. Between 500 and 200 km. distance from the center the wind profile may be represented by the relation $v_\theta r^x$ = constant, where x = 0.6 to 0.7, in agreement with the findings of Hughes [6] for a mean typhoon. Further calculations for the moderate storm are made in the next section.

Table 1. - Tangential wind speeds in moderate and intense model hurricane trajectories.

	A. Moderate	B. Intense
r (km.)	$\beta_L = 20°$; $C = -4.0 \times 10^{-8}$ cm.$^{-1}$ v_θ (m./sec.)	$\beta_L = 25°$; $C = -3.2 \times 10^{-8}$ cm.$^{-1}$ v_θ (m./sec.)
800	3.4	5.8
700	6.9	9.4
600	9.9	12.5
500	12.4	15.6
400	15.0	19.0
300	18.1	23.3
200	23.3	30.7
100	37.2	50.7
50	53.8	78.2
30	55.4	87.5

3. THE MODERATE STORM

In table 2 surface pressure, mass flow, divergence, and frictional stresses are presented for the moderate case.

For the purposes of the vertical motion and shearing stress calculations of this table, the depth of the inflow layer δz has been chosen as 1.1 km.; thus K_F in equation (5) becomes 1.5×10^{-3}. The product $v_r r$ is proportional to the ageostrophic mass inflow; v_r is calculated from $v_\theta \tan \beta$. The horizontal velocity divergence is $\frac{1}{r} \frac{\partial}{\partial r} (v_r r)$, yielding the mean vertical motion w at 1.1 km. from mass continuity. Irregular values of divergence and vertical motion occur at r = 100 km. through rapid reduction in mass flow arising from the assumption that the inflow angle β begins to decrease at that radius. This minor difficulty apart, it is seen that all strong convergence is concentrated in the core. An average ascent rate of about 30 cm./sec. or 1 km./hr. is required at the top of the inflow layer.* The surface pressure p_s was calculated from evaluating gradients over short radial intervals (10 km. in core) from equation (3) and integrating graphically, with a boundary pressure of 1011.8 mb. at r = 800 km.

*We do not regard this as a gradual layer ascent of this magnitude, but rather envisage that about 5-10 percent of the inner area is covered with updrafts of 3-6 m./sec. at this level, since recent evidence suggests that the net convergence is achieved largely by restricted ascent in a few undilute cumulonimbus towers.

Table 2. - Moderate model hurricane.

r	v_θ	v_r	β	$v_r r \cdot 10^{-9}$	$\text{div} \cdot 10^5$	w	v	τ_o	p_s
km.	m./sec.	m./sec.	degrees	c.g.s.	cm.^{-1}	cm./sec.	m./sec.	dynes/cm.^2	mb.
800	3.4	1.2	20	9.62	1	- 1.1	3.6	0.18	1011.8
700	6.9	2.5	20	17.55	0.6	- 0.66	7.3	0.71	1011.7
600	9.9	3.6	20	21.6	0.2	- 0.22	10.5	1.65	1011.5
500	12.4	4.5	20	22.5	- 0.1	+ 0.11	13.2	2.61	1011.2
400	15.0	5.5	20	22.0	- 0.65	+ 0.72	16	3.84	1010.5
300	18.1	6.6	20	19.8	- 1.1	+ 1.2	19.2	5.53	1009.5
200	23.3	8.5	20	17.0	- 2.3	+ 2.5	24.8	9.23	1007.2
100	37.2	13.5	20	13.5	-29.6	+32.6	39.6	23.5	997.7
90	40.0	11.9	17.3	10.7	-25.3	+27.9	42.0	26.5	996.0
80	42.7	10.7	14.6	8.6	-26.5	+29.7	44.2	29.3	993.8
70	46.0	9.4	11.8	6.6	-28.4	+31.3	47.2	33.4	991.0
60	49.6	7.9	9.2	4.7	-30.7	+33.8	50.3	38.0	987.35
50	53.8	6.1	6.5	3.05	-33.6	+37.0	54.0	43.8	982.4
40	57.7	3.9	3.6	1.6	-33.4	+36.7	57.9	50.2	975.35
30	55.4	1.3	1.3	0.39	-25.5	+28.0	55.4	46.0	966.0
26	39.4	0.2	0.25	0.05			39.4	25.3	962.85

The features of table 2 are realistic and consistent with presently available observations. Figures 2-4 show some comparisons. Figure 2 contains wind and pressure profiles of table 2 together with those of two medium strength hurricanes obtained by the National Hurricane Research Project; both storms were encountered between 25°-30°N. Figure 3 compares mass inflow and radial velocity distributions for these same storms with those calculated in table 2. Figure 4 shows good agreement between the shearing stresses as a function of radius calculated in table 2 with those obtained by Palmén and Riehl [14] from momentum budget requirements established from mean hurricane data.

4. PRESSURE FIELD AND OCEANIC HEAT SOURCE

As just demonstrated, pressures and pressure gradients of the moderate hurricane are similar to those observed in storms of moderate intensity such as Carrie (1957). Outward of r = 90 km. where $p_s \sim 996$ mb., the pressure field may be maintained by a mixture of the air with the characteristics of the average tropical atmosphere and varying amounts of subcloud air that has ascended in cumulus towers. The admixture of low-level air must increase inward so that at r = 90 km. the vertical temperature distribution becomes entirely controlled by the moist-adiabatic ascent. Inward of $r \sim 30$ km. or $p_s \sim 966$ mb., a sloping eye wall may be called upon to compute the excessive pressure drop often encountered just inside the eye boundary. Neither of these solutions can account for the pressure drop of approximately 30 mb. between r = 90 km. and r = 30 km. This pressure drop must be related to adiabatic ascent at increasing values of θ_E; from equation (1) θ_E of the ascending air must rise from 350° to 362.5° A. along the trajectory while the surface pressure decreases from 996 to 966 mb. Such an increase in θ_E can only be

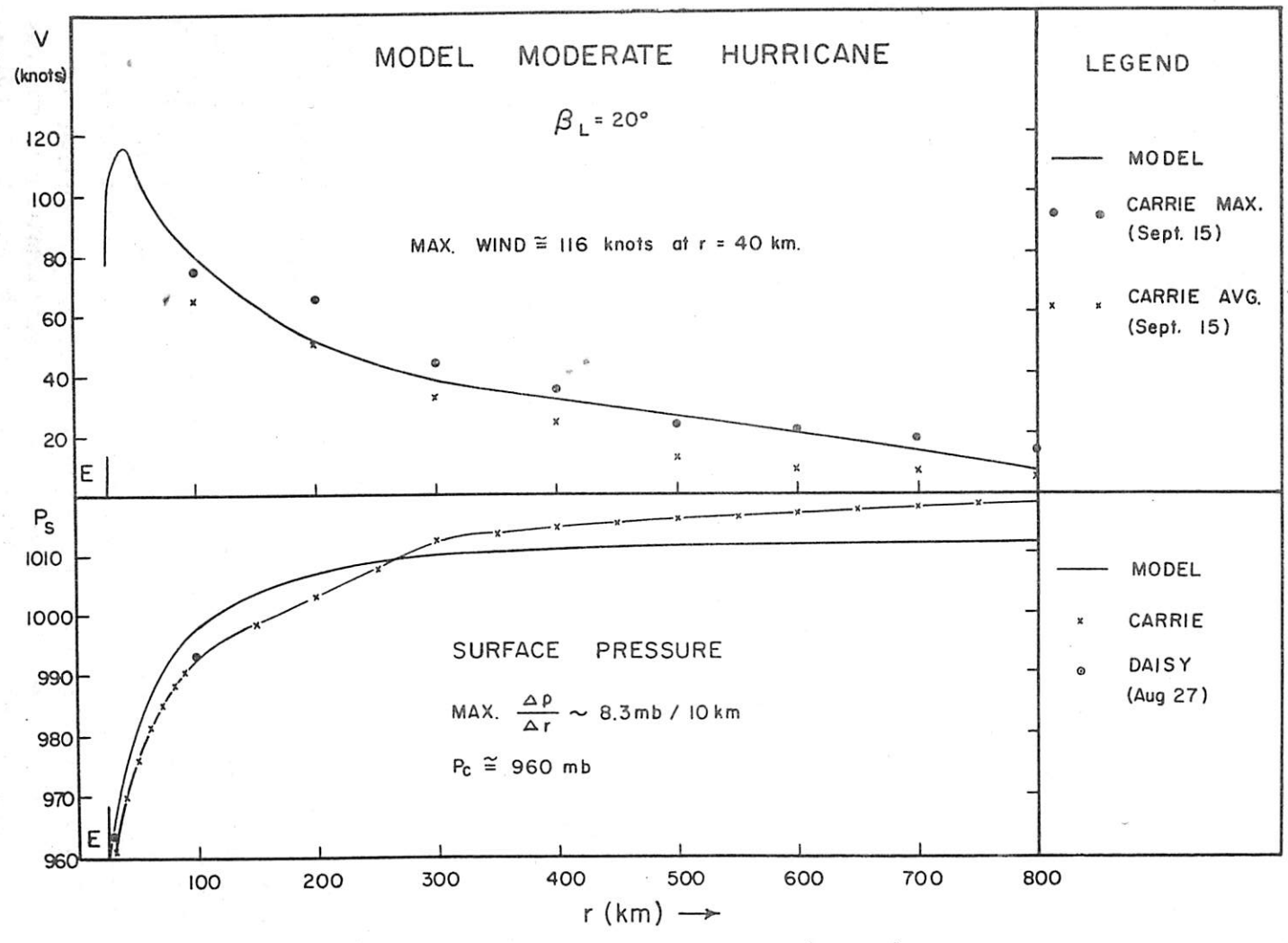

Figure 2. - Wind profile (above) and surface pressure profile (below) for model moderate storm (see table 2). Observations from actual hurricanes (Carrie, 1957, and Daisy, 1958) were provided by courtesy of the National Hurricane Research Project of the U. S. Weather Bureau. In the upper graph, circles represent the peak wind speed at each radius in Carrie, while the x's denote the radial average. In the lower graph the Carrie pressure profile is the x-ed line, while the two circles are values from Daisy.

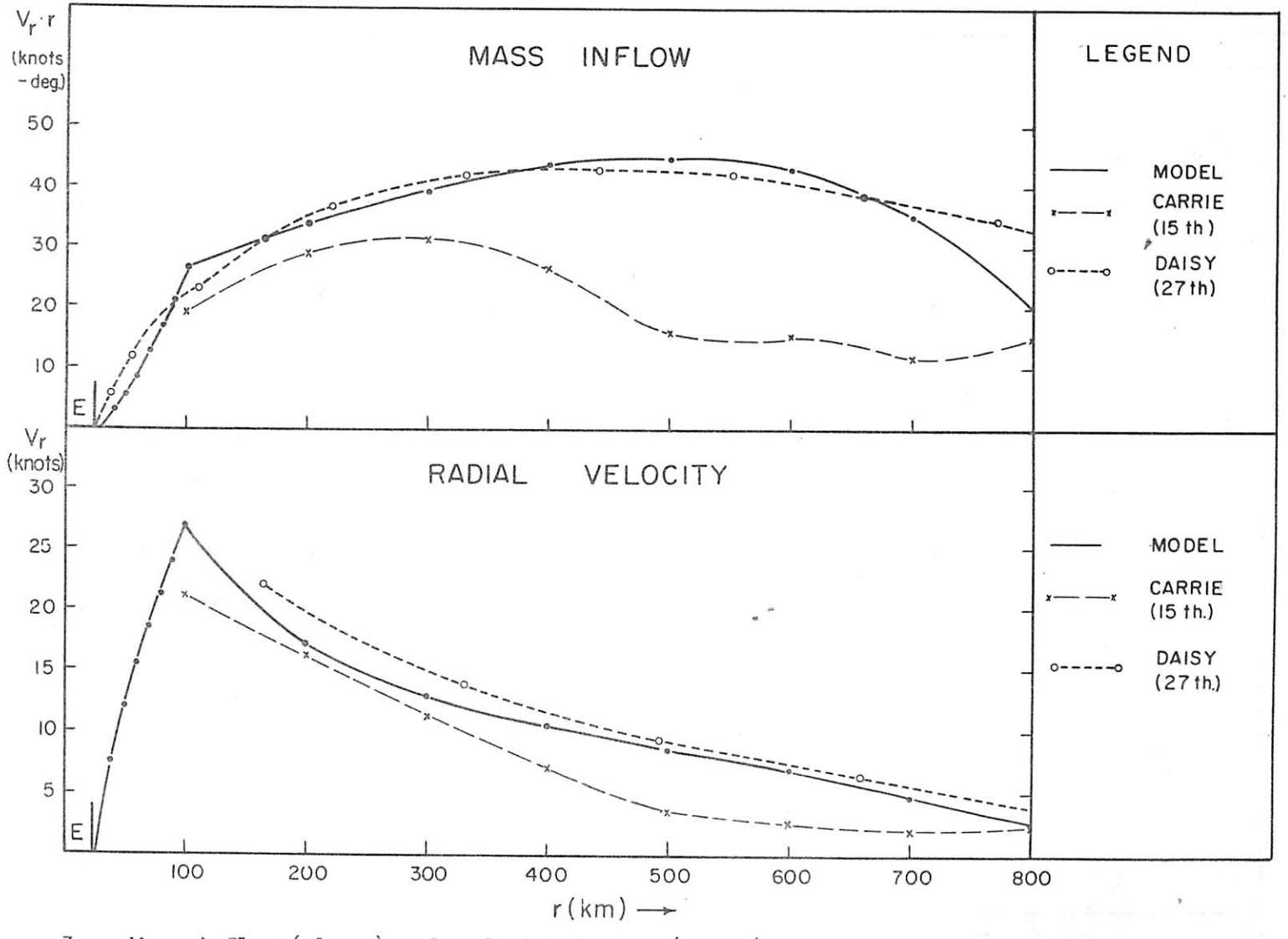

Figure 3. - Mass inflow (above) and radial velocity (below) profiles for model moderate hurricane of table 2. Dashed curves were calculated from ship observations.

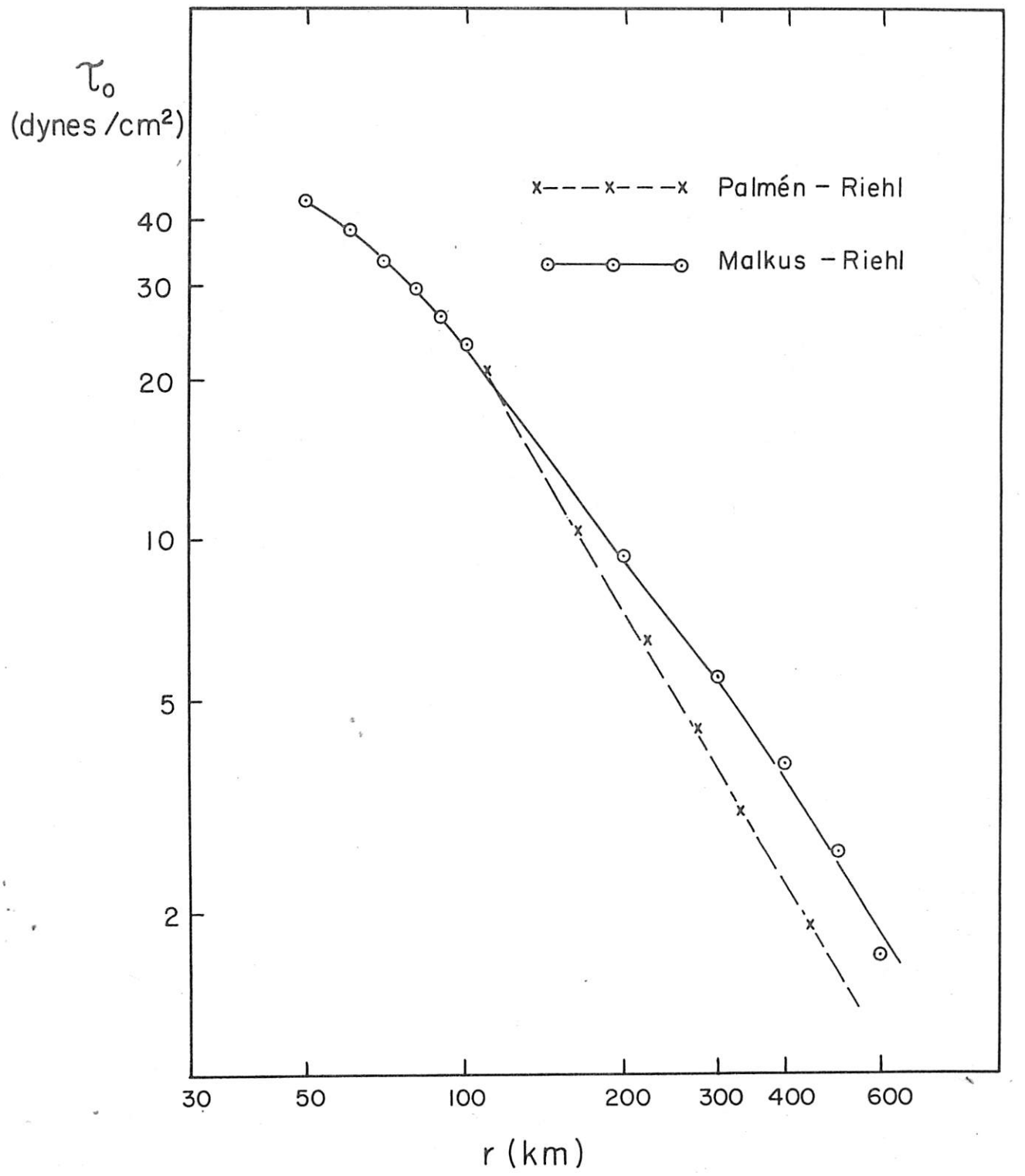

Figure 4. - Surface shearing stress (dynes/cm.^{2}) versus radius (km.). Solid curve from model moderate storm; dashed curve from momentum budgets calculated by Palmen and Riehl [14] for mean hurricane data.

obtained through a local heat source, namely transfer of sensible and latent heat from ocean to atmosphere as proposed by Byers [1] and discussed by Riehl [15].

It is the objective of this section to calculate the necessary heat exchange between sea and air and to inquire whether the ocean can supply the required heat in the available time which, from table 5, is less than three hours.

Sensible heat transfer. - In the outskirts of a hurricane the temperature of the inflowing air drops slowly due to adiabatic expansion during (horizontal) motion toward lower pressure. It is one of the remarkable observations in hurricanes that this drop ceases at pressures of 990 - 1000 mb. and that thereafter isothermal expansion takes place. Presumably, the temperature difference between sea and air attains a value large enough for the oceanic heat supply to take place at a sufficient rate to keep the temperature difference constant. In the last part of this paper, it will be shown that this corresponds to a maximum rate of conversion of the sensible heat gained to kinetic energy. For the present we shall merely utilize the fact of isothermal expansion. The first law of thermodynamics then becomes

$$dh_s = - \alpha A^* dp, \tag{11}$$

where dh_s is the sensible heat gained from the ocean, α specific volume and A^* the heat equivalent of mechanical work. Radiation may be neglected as a very small term. With use of the gas equation

$$dh_s = - RT\, d(\ln p), \tag{12}$$

where R, the gas constant for air, is expressed in heat units. Integrating over a portion of the trajectory of the surface air,

$$(h_s - h_{so})/T = R\,(\ln p_o - \ln p), \tag{13}$$

where the subscript zero denotes properties at the starting point. Given $T \sim 300°A.$, heat increments $h_s - h_{so}$ can be readily computed; for steps of 20-km. radial distance they have the values shown in table 3.

Total and latent heat transfer. - The equivalent potential temperature is defined by

$$\ln \Theta_E = \ln \Theta + Lq/c_p T \tag{14}$$

Table 3. - Sensible heat source at ocean surface.

Radial distance (km.)	70-90	50-70	30-50	30-90
$h_s - h_{so}$ (cal./gm.)	0.11	0.17	0.37	0.65

Table 4. - Oceanic heat source for moderate hurricanes.

Radial distance (km.)	70-90	50-70	30-50	30-90
Sensible heat increment (cal./gm.)	0.11	0.17	0.37	0.65
Latent heat increment (cal./gm.)	0.32	0.56	1.01	1.89
Total heat increment (cal./gm.)	0.43	0.73	1.38	2.54

where Θ is potential temperature, L latent heat of condensation, q specific humidity, and c_p specific heat at constant pressure. Since the temperature is constant

$$d(\ln \Theta_E) = d(\ln \Theta) + Ldq/c_pT, \tag{15}$$

Equation (12) may also have been written

$$dh_s = c_pT/\Theta \; d\Theta \sim c_p d\Theta \tag{16}$$

near the ground. Since dh and $d\Theta_E$ are known, equation (15) may be solved for dq. This yields the latent heat addition to the air. Table 4 shows sensible, latent, and total heat increments.

Lagrangian exchange coefficients. - One should expect that, following a particle, the heat transfer from the ocean will be governed only by the differences in temperature and vapor pressure between sea and air and wind speed. The subscript P will denote calculations performed with respect to the moving particle. Denoting sensible and latent heat transfer by Q_{SP} and Q_{eP}, we may postulate that

$$Q_{SP} = K_{SP}V\,(T_w - T_a), \tag{17}$$

$$Q_{eP} = K_{eP}V\,(e_w - e_a). \tag{18}$$

Here the subscripts w and a denote properties of the water surface and of the air, e is vapor pressure, and K_{SP} and K_{eP} are coefficients of turbulent exchange. Now $Q_{SP}dt = h_s - h_{so}$, and $Q_{eP}dt = h_e - h_{eo}$, where h_e denotes latent heat content. Integrating equations (17) and (18) from t_o to t during which time interval the particle moves the distance D along the trajectory

$$(h_s - h_{so})/D(T_w - T_a) = K_{SP}, \tag{19}$$

$$(h_e - h_{eo})/D(e_w - e_a) = K_{eP}. \tag{20}$$

The ocean temperature will be taken as 28° C., typical for the West Atlantic hurricane area, and $T_w - T_a$ will be assumed as 2°C. With this assumption, based on observations, and with equation (14) all properties of the inflowing air are given, including relative humidity and height of the cloud base. They are summarized in table 5. From equations (19) and (20) and from table 5 the values in table 6 are obtained for K_{SP} and K_{eP}.

Table 5. - Thermodynamic properties of inflow layer.

r km.	p_s mb.	θ_E °A.	θ °A.	T °C.	q gm./kg.	rh °/o	LCL m.	Δs km.	Δt min.
90	996	350	299.4	26.0	18.5	84	400		
								79.7	30
70	991	352.1	299.9	26.0	19.1	86	300		
								125.4	42
50	982.4	355.7	300.5	26.0	20.1	90	200		
								294.0	88
30	966	362.5	301.8	26.0	21.8	97	80		

Δs denotes distance along each trajectory leg, from 90 to 70 km. etc.
Δt is time needed to traverse each leg.
LCL is the lifting condensation level or cloud base height.

Table 6. - Lagrangian coefficients of turbulent exchange.

Radial distance (km.)	70-90	50-70	30-50
K_{SP} (10^{-9}cal./gm.cm.deg.)	6.9	6.8	6.3
K_{eP} (10^{-9}cal./gm.cm.mb.)	4.5	5.4	5.1

It is seen that the coefficients are constant within computational limits, hence that the air trajectory, computed purely from dynamic considerations, is consistent with the independent constraints of equations (17) and (18). The trajectory takes a course such that physically impossible demands are not placed on the thermodynamic interaction between sea and air.

In the following still another approach will be taken to investigate whether the rates of heat transfer from the sea are reasonable.

Heat energy budget for the inflow layer. - Up to now, the calculations have followed a particle on its path. Now heat flux and energy exchange between sea and air will be examined spatially. The purpose in doing this lies in the desire to compare the heat flux per $cm.^2$ of ocean surface as determined here and as estimated previously from turbulence theory and airplane measurements. For this purpose it will at first be necessary to compute a heat budget. This requires the assumption that the radial distribution of various properties following the trajectory in tables 2 and 5 may be taken as valid for means around concentric cylinders. Further, a top must be assigned to the inflow layer; it will be taken as 1.1 km., corresponding to a pressure interval of 100 mb. as in table 2.

Differentiating equation (16) with respect to time, multiplying with the density ρ and integrating over the volume V,

$$\int \rho \frac{dh}{dt} dV = c_p \int \rho \frac{d\theta}{dt} dV \tag{21}$$

The heat source $\int \rho \frac{dh}{dt} dV = Q_S$, now referred to space in contrast to Q_{SP} in equation (17). Because of the steady state $\frac{d\theta}{dt} = \mathbb{V} \cdot \nabla \theta$ where $\mathbb{V}$ is the three-dimensional velocity vector and ∇ the three-dimensional gradient operator. Then

$$c_p \int \rho \frac{d\theta}{dt} dV = c_p \int \rho \mathbb{V} \cdot \nabla \theta dV = c_p \int (\nabla \cdot \rho \mathbb{V}\theta - \theta \nabla \cdot \rho \mathbb{V}) \, dV.$$

The second term is zero from mass continuity. Applying Stokes' theorem

$$Q_S = c_p \int \rho \, c_n \, \theta d\sigma = c_p \sum_{\sigma} M_\sigma \, \theta \tag{22}$$

where σ is the surface bounding the volume V and c_n is the velocity component normal to this surface, positive outward. On the right side of the expression, actually used for calculation, M_σ is the mass flux in gm./sec. through each face σ of the box considered.

The latent heat flow may be determined from

$$d/dt \, (Lq) = \mathbb{V} \cdot \nabla \, (Lq). \tag{23}$$

After transformations corresponding to those just shown for sensible heat, the oceanic latent heat source (Q_e), also referred to space, is

$$Q_e = \int Lq \, \rho \, c_n \, d\sigma = \sum_{\sigma} L_q \, M_\sigma \tag{24}$$

The total heat source is therefore

$$Q_S + Q_e = \int (Lq + c_p \, \theta) \rho \, c_n \, d\sigma = \sum_{\sigma} (Lq + c_p \, \theta) \, M_\sigma \tag{25}$$

Radial and vertical fluxes of sensible and latent heat may be computed from the data in tables 2 and 5. These fluxes, and the heat sources required for balance are shown in tables 7 and 8 and figures 5-6. These diagrams were derived as follows: The mass flux through each vertical face (at r = 90, 70, 50, and 30 km.) was obtained from $M = v_r \, r \, 2\pi \frac{dp}{g}$, where v_r was taken from table 2. The mass flux through the top face, ΔM, is the difference between the horizontal fluxes through successive vertical faces. Mass leaving through the top of each box was assumed to go out with the mean property of the air in the box. Heat sources were calculated as residuals to meet continuity. Over the area within the core ($r < 90$ km.) of 226×10^{12} cm.^{2}, the total heat source is 5.38×10^{12} cal./sec. latent heat of water vapor and 1.60×10^{12} cal./sec. other, total of 6.98×10^{12} cal./sec. This corresponds to a heat increment of 2.50 cal./gm., within computational error of the result of table 4.

From turbulence theory (cf. Jacobs [7]) the following formulae have been determined for latent and sensible heat exchange between sea and air

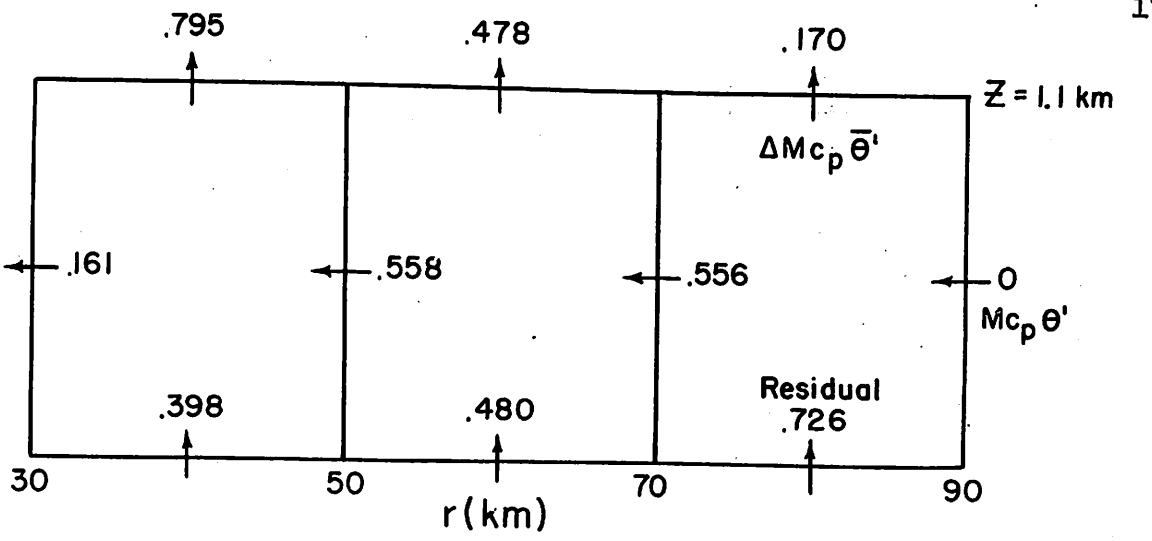

Sensible Heat Flux (10^{12}cal/sec)

Figure 5. - Sensible heat budget for moderate storm. Heat fluxes (10^{12}cal./sec.) into and out of inflow layer by boxes with Δ r = 20 km. Lateral fluxes have been calculated as shown with $\theta' = \theta - 299.4°$; for vertical fluxes it has been assumed that vertical mass flux leaves with mean θ' of interval, $\bar{\theta}'$. Input from ocean calculated as residual. Mass flows from dynamic model, table 2.

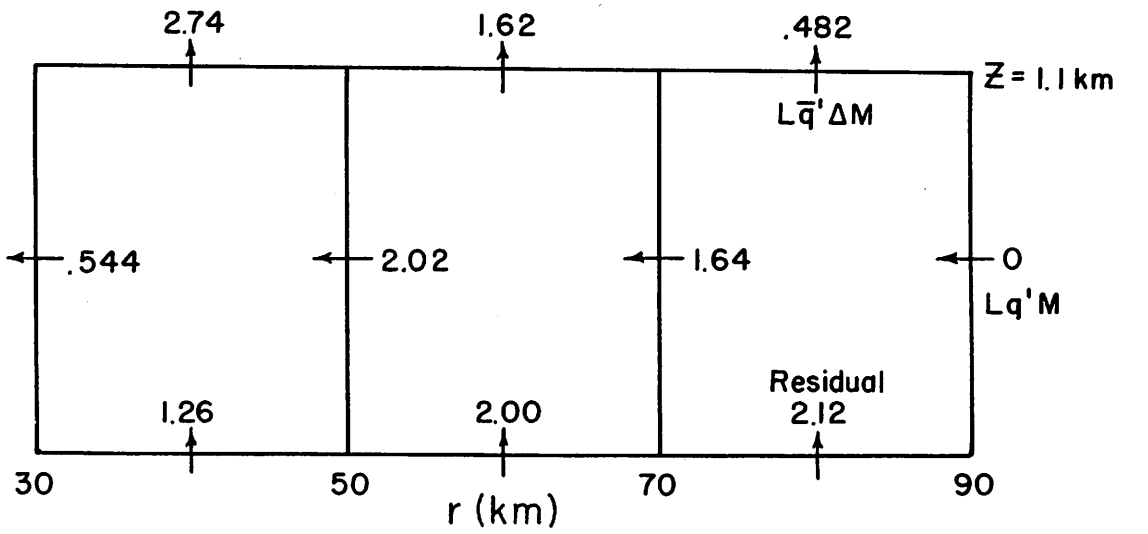

Latent Heat Flux (10^{12}cal/sec)

Figure 6. - Latent heat budget for moderate storm. Heat fluxes (10^{12}cal./sec.) into and out of inflow layer by boxes with Δ r = 20 km. Lateral fluxes have been calculated with q' = q - 18.5 gm./kg.; for vertical fluxes it has been assumed that vertical mass flux leaves with mean q' of the interval, $\bar{q}'$. Input from ocean calculated as residual. Mass flow from dynamic model, table 2.

Table 7. - Sensible heat flux.

r	θ'	M	Δ M	$M c_p \theta'$	$c_p \overline{\theta}'$	$\Delta M c_p \overline{\theta}'$
km.	°A.	10^{-12}gm./sec.	10^{-12}gm./sec.	10^{-12}cal./sec.	cal./gm.	10^{-12}cal./sec.
90	0	7.40		0		
			2.8		0.060	.170
70	0.5	4.65		0.556		
			2.5		0.191	.478
50	1.1	2.15		0.558		
			1.9		0.418	.795
30	2.4	0.28		0.161		

θ' denotes θ -299.4 and the bar indicates area averaging.

Table 8. - Latent heat flux.

r	q'	Lq'	Lq'M	$\overline{Lq'}$	$\Delta M\overline{Lq'}$
km.	gm./kg.	cal./gm.	10^{-12}cal./sec.	cal./gm.	10^{-12}cal./sec.
90	0	0	0		
				0.172	0.482
70	0.6	0.353	1.64		
				0.647	1.62
50	1.6	0.941	2.02		
				1.44	2.74
30	3.3	1.94	0.544		

q' denotes q -18.5 °/oo and the bar indicates area averaging.

$$Q_s / A = K_s (T_w - T_a) v, \tag{26}$$

$$Q_e / A = K_e L (q_w - q_a) v. \tag{27}$$

Here Q_s and Q_e are the fluxes in cal./sec. computed from equations (22) and (24) respectively; A is the area in $cm.^2$ of ocean surface; $T_w - T_a$ the difference in °C. between deck level and sea surface temperature; $q_w - q_a$ the difference in gm./gm. between the saturation specific humidity at the temperature of the sea surface and the actual specific humidity at deck level, and v is the wind speed in cm./sec. K_s and K_e are coefficients of turbulent exchange analogous to those of equations (17) and (18). But, as already stressed, the meaning of these equations is quite different because they refer to the heat flow per unit area of ocean surface. Riehl et al. [20] have used the following constants for calculation of heat exchange in the trades, based on Montgomery [13]: $K_s = 4.16 \times 10^{-7}$, $K_e = 1.71 \times 10^{-6}$. Recent direct flux

Table 9. - Constants for moderate hurricane.

r	$T_w - T_a$	$q_w - q_a$	$\bar{v}$	A	K_s	K_e	Q_s/Q_e
km.	°C.	gm./kg.	Area-Ave. m./sec.	10^{-12} cm.^{2}	10^7	10^6	per-cent
90-70	2	5.2	44	100	8.6	1.64	34
70-50	2	4.6	50	76	6.3	1.95	24
50-30	2	3.5	56	50	7.1	2.19	32
Area Ave.					7.4	1.92	30

measurements by Bunker [2] under normal and disturbed trade conditions have confirmed these values within about 25 percent. When we solve equations (26) and (27) for the constants and use the results of figures 5-6 and tables 7-8, we obtain for the hurricane the constants shown in table 9.

The most interesting result of table 9 lies in the fact that the coefficients of turbulent exchange differ very little from those for the trades. No special demand is created during transition from trade wind speeds of about 7 m.p.s. to hurricane velocities for an increase of the transport efficiency of the energy spectrum near the ground. No impossible or difficult restriction is made when it is postulated that lowering of surface pressures in hurricanes arises mainly through an 'extra' oceanic heat source in a storm's interior.

The actual transports, of course, are very large in the hurricane compared to the trades. Sensible heat pickup is 720 cal./cm.^{2}/day, an increase by a factor of 50 over the trades (Riehl et al. [20]); latent heat pickup is 2420 cal./cm.^{2}/day, higher by a factor of 12-13. The difference arises largely through the high wind speed. The fact that the inflowing air is observed to cool by about 2°C. before onset of active heating from the ocean, accounts for the larger rise in sensible heat pickup. While $q_w - q_a$ remains about constant, $T_w - T_a$ increases from a mean of about 0.5°C. in the trades over the western parts of the ocean during summer to 2°C. or more inside hurricanes.

In trade-wind disturbances it has also been noted that Q_s and Q_e are higher than in the undisturbed trades, and that the increase in Q_s is percentually larger (Garstang [4]). However, the increase of $T_w - T_a$ in this type of situation must be related to evaporation of falling rain and thunderstorm downdrafts rather than to adiabatic expansion during horizontal motion toward lower pressure. These mechanisms for lowering the air temperature need not be discounted in hurricane circulations, especially in the outskirts at pressures above 1000 mb. As calculated by Riehl and Malkus [19], re-cycling of air at upper levels to the surface by means of cumulonimbus downdrafts makes

an important contribution to the heat budget of the equatorial trough zone, especially to the pickup of sensible heat from the ground. For this region the ratio Q_s / Q_e was found to be 0.4, compared to estimates of 0.05 - 0.1 for the trades at large, and compared to 0.3 for the hurricane from tables 4 and 9.

5. THERMAL CONSTRAINTS, RELATIVE STABILITY, AND CONDITIONS FOR EXTREME STORMS

The solutions to the dynamic equations for the hurricane inflow layer contain a parameter $C = \frac{-K_F}{\sin\beta\,\delta z}$, variations in which give rise to an infinite family of logarithmic spiral trajectories for each choice of boundary condition r_o. We saw from table 1 that when r_o = 500 km., a choice of $C = -4.0 \times 10^{-8}$ cm.$^{-1}$ gave a moderate storm with maximum wind of 110 knots, while a choice of $C = -3.2 \times 10^{-8}$ cm.$^{-1}$ gave an intense storm with maximum wind of 175 knots.

It is the purpose of this section to suggest that the thermal constraints which, in nature, operate upon the system in addition to the dynamic ones impose a choice between, or a limit upon, the range of dynamically possible trajectories so that most or even all of these may be prevented from occurring in a real situation. We shall show that the thermal constraints operate through the surface pressure gradient along s in the storm core and that the realizable $\frac{\partial p}{\partial s}$ is restricted by the possible heat transfer at the air-sea boundary and by the thermodynamics of the condensation heat release in the vertical.

In section 4, the pressure reduction following a parcel along an inflow trajectory was related to the sensible heat transfer from the ocean using the first law of thermodynamics (equation (11)) in the form that obtains if heat is added at constant temperature. As mentioned, this implies maximum production of kinetic energy through the sensible heat source. When equation (11) is differentiated with respect to time,

$$J \frac{dh_s}{dt} = -\frac{1}{\rho} \frac{dp}{dt}, \tag{28}$$

where J is the mechanical equivalent of heat. For particles moving horizontally toward the center

$$\frac{1}{\rho} \frac{dp}{dt} = \frac{v}{\rho} \frac{\partial p}{\partial s} \tag{29}$$

The well-known kinetic energy equation is obtained by multiplying equation (2) by v,

$$v \frac{dv}{dt} = -\frac{v}{\rho} \frac{\partial p}{\partial s} + \frac{v}{\rho} \frac{\partial \tau_{sz}}{\partial z} \tag{30}$$

The term $-\frac{v}{\rho} \frac{\partial p}{\partial s}$ is the production of kinetic energy by pressure forces, and it is now apparent that kinetic energy is produced from the oceanic heat source at a maximum rate during isothermal and horizontal motion.

From equations (17), (28), and (29) the pressure gradient force may be related explicitly to boundary heat transfers,

$$J \frac{dh_s}{dt} = JQ_{SP} = JK_{SP} (T_w - T_a)v = - \frac{v}{\rho} \frac{\partial p}{\partial s} ,$$

so that

$$- \frac{1}{\rho} \frac{\partial p}{\partial s} = JK_{SP} (T_w - T_a) \tag{31}$$

The pressure gradient along the trajectory is thus limited by the input rate of sensible heat from sea to air.

A second thermal constraint must be met by the system. Since hydrostatic equilibrium prevails, pressures exerted by and on subcloud air particles must be consistent with the density of the air column above them. If the lapse rate is essentially wet adiabatic, equation (1) relates the surface pressure to the equivalent potential temperature θ_E of the vertical column. This places a simultaneous constraint upon the total, latent plus sensible, heat addition.

From equation (1)

$$\frac{\partial p}{\partial s} = - \mathcal{H} \frac{\partial \theta_E}{\partial s} \tag{32}$$

where $\mathcal{H} = 2.5$ mb./°A.

Furthermore,

$$\frac{d\theta_E}{dt} = v \frac{\partial \theta_E}{\partial s} \cong \frac{Q_{SP} + Q_{eP}}{c_p} . \tag{33}$$

Combining (32) and (33) and substituting from (18), we have

$$- \frac{1}{\rho} \frac{\partial p}{\partial s} = \frac{\mathcal{H}}{v} \frac{1}{\rho c_p} (Q_{SP} + Q_{eP}) = \frac{\mathcal{H}}{\rho c_p} [K_{SP}(T_w - T_a) + K_{eP}(e_w - e_a)]$$

To be consistent with (31)

$$K_{SP} (T_w - T_a) = \frac{\mathcal{H}}{\rho c_p} [K_{SP} (T_w - T_a) + K_{eP} (e_w - e_a)] \tag{34}$$

and a relation between sensible and latent heat pick-up is prescribed. With the data of section 4, $Q_{SP} = 1/3\ Q_{eP}$ from equation (34) for the moderate storm.

Maximum kinetic energy production and relative stability criterion. - As shown, the core surface pressure gradient is restricted by thermal processes, sea-air transfer on a turbulent-convective scale and condensation heating on a convective cloud scale. These operate to limit the realizable values of C and thus impose a restriction upon the selection of actual trajectory. The upper limit may be calculated, based on a thermal circulation theory by W. Malkus and Veronis [11]. They showed that when several solutions to the equations of motion are possible, that one is selected which maximizes, under the thermodynamic constraints, the kinetic energy production, or strictly, potential energy release minus frictional dissipation of kinetic energy. The theory

takes the form of a "relative stability" criterion. It is rigorous if production and dissipation terms, and constraints, can be stated formally in the kinetic energy equation.

If equation (30) is integrated vertically through the inflow layer with the assumptions and methods applied to equation (4)

$$\frac{dK}{dt} = \frac{1}{2}\frac{dv^2}{dt} = -\frac{v}{\rho}\frac{\partial p}{\partial s} - \frac{K_F}{\delta z}v^3 , \qquad (35)$$

where K is kinetic energy per unit mass. Following Malkus and Veronis, we shall substitute the dynamic solution for v as a function of C (equation (9)) into (35) and maximize dK/dt as a function of C. The weakness of the approach relative to that of Malkus and Veronis is that we are as yet unable to formulate the constraints rigorously. All dissipation of kinetic energy is incorporated into friction at the boundary in terms of an empirical coefficient K_F. The pressure production term we believe to be limited by boundary transfers and cloud-scale releases; clearly these may depend upon the dynamics in a manner as yet unknown. Nevertheless, the results are of interest and point the direction for further investigation.

The maximization of dK/dt as a function of C in equation (35) will be carried out at $r = r_1 = 100$ km., where the core pressure gradients maintain and where the angle β is still assumed constant at β_L. Selection of β at this radius (together with r_o) completely determines the dynamic solution. When $-\frac{1}{\rho}\frac{\partial p}{\partial s}$ from equation (31) is substituted into (35), the latter equation has the form

$$dK/dt = A\, v_1 - B\, v_1^3$$

where $v = v_1$ at r_1, $A = -\frac{1}{\rho}\frac{\partial p}{\partial s} = JK_{SP}(T_w - T_a)$ and $B = K_F/\delta z$. dK/dt is an implicit function of C through equation (9). Differentiating with respect to v_1 and equating the derivative to zero, we find the value of v_1 which maximizes dK/dt, namely

$$d/dv_1\,(dK/dt) = A - 3Bv_1^2 = 0,$$

and

$$v_{1m} = \sqrt{\frac{A}{3B}} = \sqrt{\frac{JK_{SP}(T_w - T_a)}{3K_F/\delta z}} \qquad (36)$$

where v_{1m} is the value of v_1 which maximizes dK/dt. Substitution from equation (9) for v in terms of C permits solution for the maximum constant C_m when $K_{SP}(T_w - T_a)$ and the other parameters are prescribed. In general, this leads to a transcendental equation in C_m which had to be solved numerically. The procedure will be illustrated for the case where $r_o \geq 800$ km. so that the exponential term in equation (9) is negligible, with the approximation that

$v \sim v_\theta$ which for kinetic energy considerations is very nearly true. Then equation (9) becomes

$$v_{lm} = \frac{f}{C_m^2 r_l} [1 - C_m r_l]. \tag{37}$$

Combining (36) and (37)

$$C_m^2 r_l \sqrt{\frac{JK_{SP}(T_w - T_a)}{3K_F/\delta z}} + fC_m r_l - f = 0 \tag{38}$$

If we substitute the values of $JK_{SP}(T_w - T_a)$ calculated from table 3 for the moderate storm, and also the values of the other parameters assumed for the model, $C_m = -4.35 \times 10^{-8}$ cm.$^{-1}$ and $\beta = 18°10'$. Using the exact equation (9), $C_m = -4.0 \times 10^{-8}$ cm.$^{-1}$ or $\beta = 20°$ for $r_o = 500$ km.

Figure 7 shows the result of the calculation. The solid lines denote v as a function of C at 100 km. for different values of r_o. The x's on these curves were arrived at by the relative stability criterion using the exact equation (9) and various values of $JK_{SP}(T_w - T_a)$. These are entered in terms of $-\frac{1}{\rho}\frac{\partial p}{\partial s}$ (by equation (31)) in the figure, with dashed lines interpolated to show what points would be chosen on dynamic curves intermediate between those actually drawn. We see that for the intense storm ($r_o = 500$ km.; $C = -3.2 \times 10^{-8}$) $-\frac{1}{\rho}\frac{\partial p}{\partial s}$ in the core must be about 1.44 cm./sec.^{2} or 2.4 times that of the moderate storm, which means that the product $JK_{SP}(T_w - T_a)$ must be 2.4 times greater as well as the sum of $Q_{SP} + Q_{eP}$. We do not yet know whether there is an upper limit upon $T_w - T_a$ and $e_w - e_a$, which for example might be imposed by the dewpoint of the inflowing air.

The criterion of maximum rate of kinetic energy production within the thermal constraints of the system would determine, if we could formulate the latter rigorously, the selection between dynamically possible trajectories. Actually we have said only how the heat must be transferred and released to realize these and must look further into the controls upon convective and turbulent scale processes and their interaction with large-scale dynamics. However, once $\frac{1}{\rho}\frac{\partial p}{\partial s}$ (core) and r_o determine β, a relatively simple method for estimating the strongest wind within the core is available from formulation and integration of equation (35) with respect to s, namely

$$\frac{1}{2}\frac{dv^2}{ds} + \frac{K_F}{\delta z} v^2 = -\frac{1}{\rho}\frac{\partial p}{\partial s} = K_{SP}(T_w - T_a) \tag{39}$$

when dv/dt is written v dv/ds and a v is divided out.

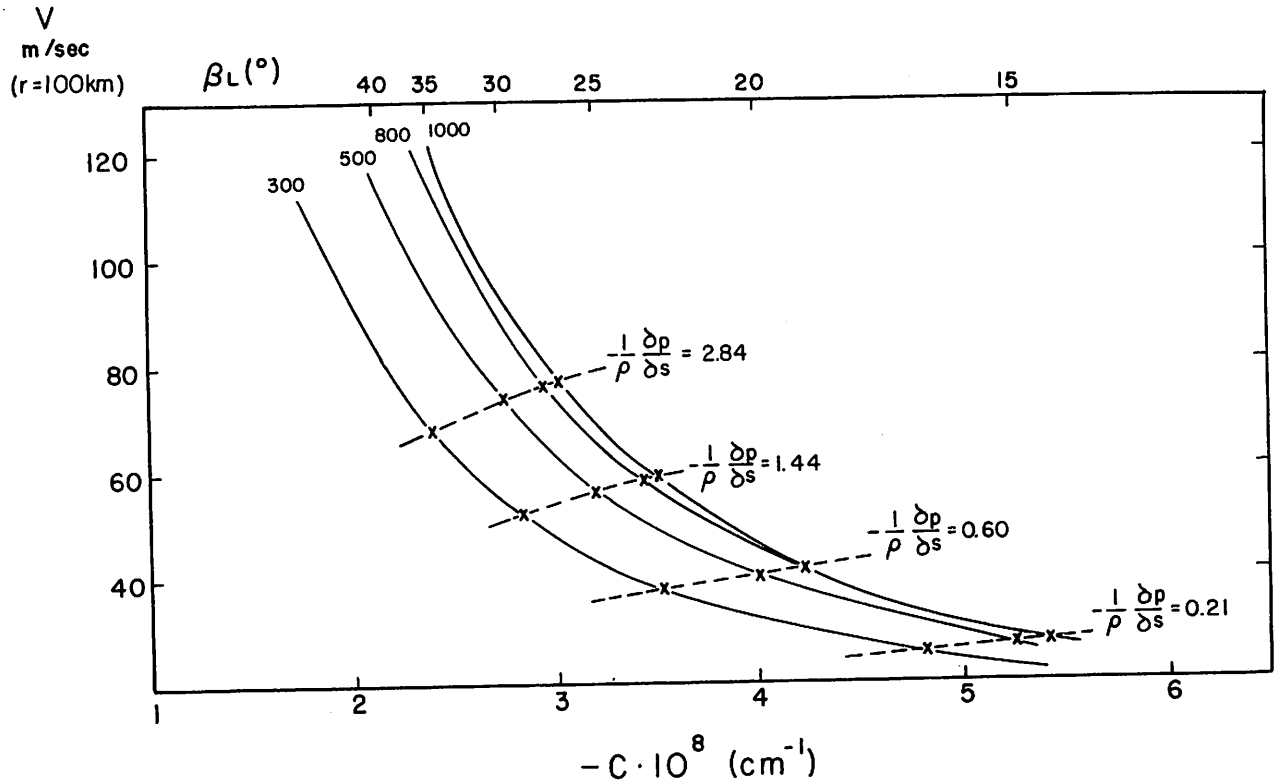

Figure 7. - Graph showing results of trajectory selection by relative stability criterion. Calculation made at r = 100 km. Solid lines show relationship between v in m./sec. (ordinate) as function of -C(r) (abscissa) when r_o is chosen as labelled at the left of each solid curve. For a single choice of r_o, these dynamic solutions permit an infinity of v's at 100 km. depending on choice of C. The x's show how the relative stability (maximum kinetic energy production) criterion selects only one of these when the core pressure gradient $-\frac{1}{\rho}\partial p/\partial s$ is prescribed. Fixing $-\frac{1}{\rho}\partial p/\partial s$ chooses from curve only one possible solution, indicated by intersection of dashed and solid lines.

The solution is

$$v^2 = v_o^2 e^{-\frac{2K_F S}{\delta z}} + \frac{K_{SP}(T_w - T_a)\delta z}{K_F}\left(1 - e^{-\frac{2K_F S}{\delta z}}\right) \qquad (40)$$

with $v = v_o$ at $s = 0$, which is to be the value of v at r = 100 km. Figure 8 gives the results for the moderate and intense storms. The comparison with the v's (points in fig. 8) calculated from equation (10) is, as expected from table 6, excellent except in the inmost regions, showing that the arbitrary linear decrease in $\sin\beta$ with radius in the core is a fair approximation to maximum kinetic energy production at first, but decreases the inflow angle too rapidly near the eye wall.

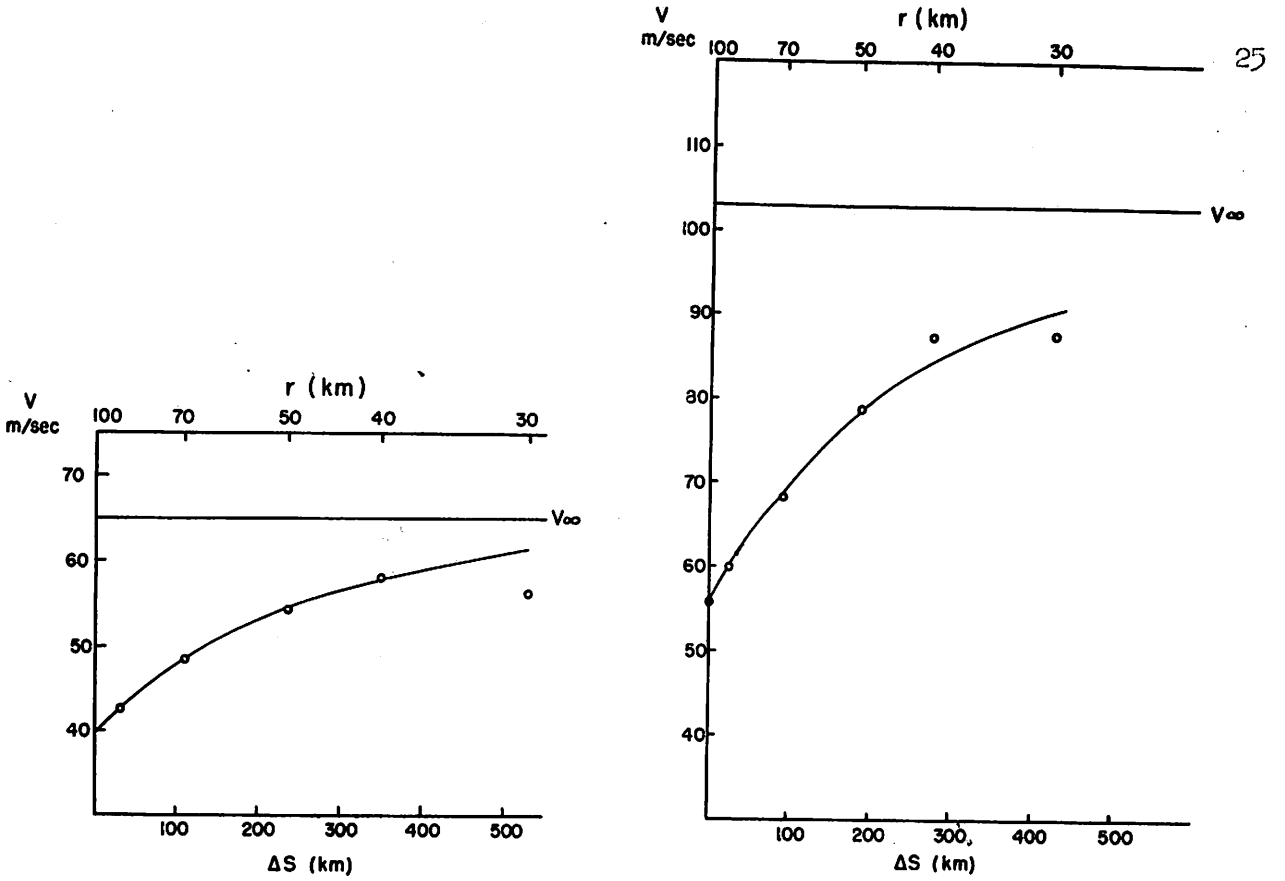

Figure 8. - Core velocity (m./sec.) as function of r and Δ s (distance along trajectory from r = 100 km.); A for moderate storm, B for intense storm. Solid curves show profile from solution to equation (39) representing maximum kinetic energy production, with $-\frac{1}{\rho}\partial p/\partial s$ chosen as prescribed by figure 7. Points are values from dynamic model via equations (9) and (10).

Equation (40) shows that as s becomes large, the velocity asymptotically approaches a limiting value, called v_{∞} in figure 8, namely

$$v_{\infty} = \sqrt{\frac{K_{SP}(T_w - T_a)\,\delta z}{K_F}} \qquad (41)$$

which is determined by heat transfer (or core pressure gradient along s) and the ratio of depth of inflow layer to surface friction coefficient only. For the moderate storm, v_{∞} has the value 66.5 m./sec. and for the intense storm it is 106 m./sec. For the normal range of inflow angles considered, the maximum wind attained just outside the eye wall is about 90 percent of v_{∞}. Therefore if we know the velocity and inflow angle (radial average) at r = 100 km., we can read from figure 7 the core value of $-\frac{1}{\rho}\frac{\partial p}{\partial s} = JK_{SP}(T_w - T_a)$ and estimate the maximum wind speed from the relation

$$v_{max} = 0.9\sqrt{\frac{K_{SP}(T_w - T_a)\delta z}{K_F}} \qquad (42)$$

Conditions for extreme storms. - We may now inquire into conditions for an extreme storm with maximum winds on the order to 200 knots and central pressures below 900 mb. From equation (42) a core pressure gradient of 2.0 cm./sec.^{2} (3.4 times that of the moderate storm) produces a maximum wind of about 105 m./sec. or 210 knots. Using figure 7, such a storm will be obtained with $\beta_L = 25°$, $r_o = 800$ km. A dynamic calculation was carried out for this storm, in the same manner as for the previous two. At latitude 20°, a hurricane for which this trajectory is a mean would need a central pressure of 882 mb., about as low as any hurricane or typhoon pressure on record. The requirements of moderate, intense, and extreme storm are compared in table 10.

To maintain hydrostatically the extreme pressure of 882 mb., the required θ_E is 396°A. from equation (1). Although pressures above the 100-mb. level must be somewhat disturbed by such a deep storm and ascents of this heat content, this would not occur unless $\theta_E \geq 395°A$. Ascent with this very high heat content is possible if subcloud air is heated isothermally at T = 28.2°C. and the specific humidity is 27 gm./kg. (cloud base $\sim$100 m.). If the sea surface temperature is about 30°C., the same air-sea temperature and vapor pressure differences are obtained as used in section 4 for the moderate storm. Thus, in the framework of this model, to achieve the extreme storm, transfer coefficients enhanced by a factor of 3-4 appear to be necessary. That central typhoon pressures approaching these values have been observed suggests this is possible.

There are thus two simultaneous thermal constraints which restrict the solution to the dynamics of the hurricane inflow. The first is set by the air-sea boundary and the sensible heat transfer, the second by the boundary latent heat transfer and the ability of the atmosphere to convert the latent to sensible heat by wet adiabatic ascent. During deepening of a storm to moderate intensity it appears that the latter restriction is usually the binding one, in that super-normal transfer rates per property difference and wind speed are not required. During deepening to the extreme strength, the boundary constraints may become predominant, for transfer coefficients be enhanced several factors above normal may be required.

In conclusion of this section, we see that higher average inflow angles, or more exactly lower values of C, permit more intense storms due to reduction of trajectory distance and thereby of frictional dissipation of kinetic energy.

Table 10. - Comparison of moderate, intense, and extreme hurricane.

Storm	β_L	r_o	v_{max}	$(-\frac{1}{\rho}\frac{\partial p}{\partial s})_{core}$	Ratio core press. grad. to moderate storm	p_c	θ_E(max)
	(deg.)	(km.)	(m./sec.)	(cm./sec.^{2})		(mb.)	(°A)
A. Moderate	20	500	60	0.6	1.0	966	362.5
B. Intense	25	500	90	1.44	2.4	910	385
C. Extreme	25	800	105	2.0	3.4	882	396

Table 11. - Precipitation and efficiency of hurricane circulations.

Storm	$\overline{R}$ Rainfall 90-30 km. cm./day	$\overline{H}$ Latent heat release joules/sec. 10^{12}	$\overline{GF}$ Ground friction joules/sec. 10^{12}	Efficiency $\overline{GF}/\overline{H}$ percent	$\overline{PW}$ Pressure-work joules/sec. 10^{12}	Production $\overline{PW} - \overline{GF}$ joules/sec. 10^{12}
A. Moderate	48	272	3.7	1.4	6.6	2.9
B. Intense	78	443	11.7	2.6	22.8	11.1
C. Extreme	94.5	535	17.6	3.3	36.2	18.6

— denotes area average between r = 90 km. and r = 30 km.

The larger the inflow angle, the closer the velocity profile approaches that of the constant angular momentum vortex which, without friction, would arise from any inflow angle. Very high angles are prevented in real situations due to thermodynamic restrictions on the realizable pressure gradients. When the trajectory distance is reduced, the air cannot pick up and release by condensation enough extra heat energy to achieve the required gradient of Θ_E and thus of surface pressure. In each hurricane situation there is a balance whereby the trajectory adjusts its angle so that just enough heat is supplied and released to maintain the pressure gradients that the resulting dynamic fields require.

6. RAINFALL AND KINETIC ENERGY

It is desirable to determine whether the models evolved permit precipitation in the amounts commonly observed in hurricanes, and what the efficiency of the latent heat release must be in this type of thermal engine. We may estimate the area-averaged precipitation in the cores of storms A, B, and C, following the method of Riehl and Byers [16]. The method consists in determining the difference in moisture import between r = 90 km. and r = 30 km. and assuming that this amount of vapor is lifted and condensed. If the storm outflow occurs high enough so that 75 percent of the converging vapor is precipitated and only 25 percent or less is exported in the upper outflow, the figures of table 11 are obtained.

Determination of the radial velocity from dynamic calculation gives the mass flow as a function of radius for any chosen depth of the inflow layer. The latter is assumed here to extend over a pressure depth of 100 mb., a low estimate. In actual cases, some inflow has been observed to occur as high as the middle troposphere. Mixing ratios are obtained from the data of section 4. The rainfall of 48 cm./day inside the 90-km. radius for the moderate storm agrees favorably with the average of 33.7 cm./day in the inner 1°-latitude (111-km.) radius quoted by Riehl [15], where the same inflow depth was used, and with the order of magnitude of precipitation observed in hurricanes. The column in table 11 labelled latent heat release is computed directly from the amount of precipitation.

We may inquire about the relative magnitude of the latent heat release compared to the frictional kinetic energy dissipation in the core to estimate the storm's "efficiency" as defined by Riehl and Byers [16], Defant [3], and others.

The dissipation of kinetic energy by ground friction (GF) may be obtained from the expression

$$\overline{GF} = -K_F \rho_o \overline{v_o^3} A,$$

where $A = 2.26 \times 10^{14}$ cm.^{2} is the area between r = 90 km. and r = 30 km., and $\overline{v_o^3}$ is the area average of the cube of the wind speed. Alternately, $\overline{GF}$ may be computed from equation (35) by multiplying $\overline{v_o^3}$ therein by the mass in the core. The results for $\overline{GF}$ and the efficiency of the circulation defined as $\overline{GF}/\overline{H}$ are shown in table 11. It is interesting to note that the more intense storms require a more efficient release of latent heat, due to the increase of $\overline{GF}$ with the cube of v, while the moisture convergence increases approximately as v.

The last two columns in table 11 give the area-averaged pressure work, and the difference between kinetic energy production and dissipation by ground friction for the inflow layer. These columns were obtained from equation (35) taking area-averages of v and v^3 and multiplying by the mass. It is seen that the production rate is roughly twice the dissipation rate for all three storms. Since steady-state hurricanes are considered, the dissipation of kinetic energy by internal friction must at least equal the boundary dissipation. Normally the wind speed is much higher in the inflow layer at r = 90 km. than in the high-tropospheric outflow layer, so that kinetic energy is imported from the outer regions of a hurricane toward the core. This implies that internal may exceed the boundary dissipation. A more complete kinetic energy budget for the moderate storm is computed in the following.

The kinetic energy budget for the core region of the moderate storm is shown in figure 9, broken down into the same intervals as the heat and moisture budget was in section 4. The horizontal imports and exports through vertical walls were calculated by multiplying the kinetic energy per unit mass, $v^2/2$, with the radial mass flow. Similarly, the flux through the top of the layer was determined by multiplying the area average of $v^2/2$ for each increment of 20 km. in radius with the vertical mass flow for each of the three areas. The boundary dissipation GF was calculated as residual; total GF coincides with that of table 11. This agreement supports the calculations of table 11 materially, because an arbitrary coefficient K_F need not be assumed for figure 9.

It is seen that the pressure work PW exceeds GF in each interval but by decreasing amounts as the center is approached. Total production for the whole area is 66.3 units, almost the same as the import through the outer boundary. Thus a major fraction of the kinetic energy of a hurricane is produced outside its core (cf. also Palmén and Riehl [14]).

It would, however, be misleading to deduce that the core is maintained chiefly by importation of kinetic energy produced in the outskirts. To illustrate this, the budget of figure 9 may be recomputed equating GF = PW in the intervals 90-70 km. and 70-50 km. Given the requirement that the vertical export be at the value of $\overline{v^2}$, we have a wind speed of only 34 m./sec. at

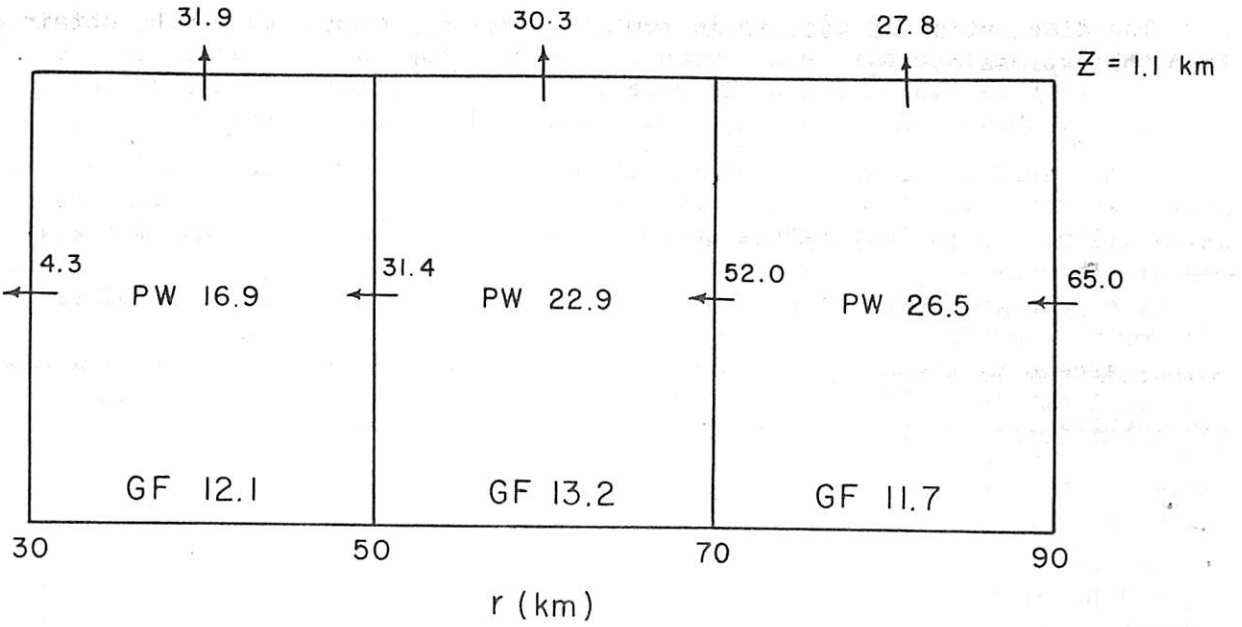

Figure 9. - Kinetic energy budget of inflow layer for moderate storm computed by same radial intervals as figures 5 and 6. Unit 10^{11} joules/sec. The term PW denotes work done by pressure forces, GF dissipation of kinetic energy by ground friction. The terms with arrows indicate lateral and vertical transports.

r = 50 km., and a minimal strength hurricane with a maximum wind of 42 m./sec. at r = 70 km. Further, as shown by Riehl and Gentry [18], non-hurricane tropical storms may possess total kinetic energies comparable to that of small hurricanes, with maximum winds at a great distance (about 150 n.mi.) from the center. What these storms apparently do not possess is the core production necessary to accelerate the small amount of mass penetrating to the center to high speeds. Therefore, an essential ingredient determining the difference between tropical storm and hurricane appears to be the core production which in turn depends on the extra oceanic heat source and the release of the latent heat at high θ_E.

The kinetic energy transported through the top of the inflow layer in figure 9 will in small measure be exported by the outflow; the latter may also move slightly toward higher pressure above the hurricane core. However, the bulk of the kinetic energy is likely to be dissipated by internal friction over the depth of the troposphere.

7. CONCLUDING REMARKS

Some aspects of the model proposed here have been subjected to observational test, using data from flights of the National Hurricane Research Project. In particular, it was desired to learn how closely realized was the hierarchy of wet adiabatic ascents postulated to maintain surface pressure gradients. Hydrostatic calculations were undertaken for the rather complete set of flights

into hurricane Daisy (1958); while temperatures 1-3° colder than wet adiabatic ascent of surface air were common in the mid-tropospheric levels of the core, the high levels of the storm were found to be filled with air of the required θ_E. Since the hydrostatic calculations demonstrated that about 75 percent of the surface pressure lowering is achieved by warming above 500 mb., the mid-tropospheric low temperatures have a negligibly small effect on the mass distribution. These temperature deficiencies suggest, however, that the moist adiabatic ascent does not take place by means of uniform and gradual ascent of the whole mass in the hurricane but, that as postulated by Riehl and Malkus [19] for the equatorial trough zone, it is largely concentrated in regions of rapidly ascending buoyant hot towers. This subject is being developed further in current studies, which also include heat, mass, and energy budgets for observed hurricanes to be used in comparison with the present results.

ACKNOWLEDGMENTS

The writers gratefully acknowledge the support and cooperation by the National Hurricane Research Project of the U. S. Weather Bureau and its staff at every stage of the present work. Without the body of knowledge and trained personnel developed by this group, attempts to test analyses such as the present one with observations would be impossible. The former Director of the Project, Mr. R.H.Simpson, has generously contributed his support and extensive experience in hurricane studies throughout the investigation.

This research was supported by contracts of the Office of Naval Research and the U. S. Weather Bureau with the Woods Hole Oceanographic Institution and the University of Chicago.

REFERENCES

1. H. R. Byers, General Meteorology, 2nd Ed., McGraw-Hill Book Co., New York, 1944, 645 pp.
2. A. F. Bunker, Latent and Sensible Heat Flows in Air Flowing Southward over the Western North Atlantic, Contribution No. 1031 from the Woods Hole Oceanographic Institution, 1959. To be published in Journal of Meteorology.
3. A. and F. Defant, Physikalische Dynamik der Atmosphäre, Akademische Verlagsgesellschaft M.B.H., Frankfurt Am Main, 1958, 527 pp.
4. M. Garstang, Some Meteorological Aspects of the Low-latitude Tropical Western Atlantic, Results of Crawford Cruise No. 15, Woods Hole Oceanographic Institution, Ref. No. 58-42, 1958.(Unpublished manuscript.)
5. B. Haurwitz, "The Height of Tropical Cyclones and of the 'Eye' of the Storm," Monthly Weather Review, vol. 63, No. 2, February 1935, pp. 45-49.
6. L. A. Hughes, "On the Low-level Wind Structure of Tropical Storms,"Journal of Meteorology, vol. 9, No. 6, December 1952, pp. 422-428.
7. W. C. Jacobs, "On the Energy Exchange between Sea and Atmosphere," Journal of Marine Research, vol. 5, 1942, pp. 37-66.
8. C. L. Jordan, "A Mean Atmosphere for the West Indies Area," National Hurricane Research Project Report No. 6, Washington, D. C. 1957, 17 pp.
9. J. S. Malkus, "On the Maintenance of the Trade Winds," Tellus, vol. 8, 1956, pp. 335-350.
10. J. S. Malkus, "On the Structure and Maintenance of the Mature Hurricane Eye," Journal of Meteorology, vol. 15, 1958 pp. 337-349.

11. W.V.R. Malkus and G. Veronis, "Finite Amplitude Cellular Convection," Journal of Fluid Mechanics, vol. 4, 1958.
12. R. H. Maynard, "Radar and Weather," Journal of Meteorology, vol. 2, 1945, pp. 214-226.
13. R. B. Montgomery, "Vertical Eddy Flux of Heat in the Atmosphere," Journal of Meteorology, vol. 5, 1948, pp. 265-274.
14. E. Palmén and H. Riehl, "Budget of Angular Momentum and Energy in Tropical Cyclones," Journal of Meteorology, vol. 14, 1957, pp. 150-159.
15. H. Riehl, Tropical Meteorology, McGraw-Hill Book Co., New York, 1954, 392 pp.
16. H. Riehl and H. R. Byers, Flood rains in the Bocono Basin, Venezuela, Report prepared for R. J. Tipton Assoc. Engineers, 1958, 57 pp. (On file Univ. of Chicago.)
17. H. Riehl and D. Fultz, "Jet Streams and Long Waves in a Steady Rotating Dishpan Experiment: Structure of Circulation," Quarterly Journal of the Royal Meteorological Society, vol. 83, 1957, pp. 215-231.
18. H. Riehl and R. C. Gentry, "Analysis of Tropical Storm Frieda, 1957 - A preliminary report," National Hurricane Research Project Report No. 17, Washington, D. C., 1958, 16 pp.
19. H. Riehl and J. S. Malkus, "On the Heat Balance in the Equatorial Trough Zone," Geophysica, vol. 6, No. 3-4, Meteorology, 1959, pp. 503-538.
20. H. Riehl, T. C. Yeh, J. S. Malkus, and N. E. LaSeur, "The Northeast Trade of the Pacific Ocean," Quarterly Journal of the Royal Meteorological Society, vol. 77, 1951, pp. 598-626.
21. R. H. Simpson and H. Riehl, "Mid-tropospheric Ventilation as a Constraint on Hurricane Development and Maintenance," Proceedings of the Technical Conference on Hurricanes, American Meteorological Society, 1958, D41-10.
22. H. Wexler, "Structure of Hurricanes as Determined by Radar," Annals of the New York Academy of Science, vol. 48, 1947, pp. 821-844.

USCOMM-WB-DC